Machine Vision and Applications (2004) 15: 115–120
Digital Object Identifier (DOI) 10.1007/s00138-004-0136-7

Machine Vision and Applications

Deformation visual inspection of industrial parts with image sequence

Yongjun Zhang, Zuxun Zhang, Jianqing Zhang

School of Remote Sensing and Information Engineering, Wuhan University, Wuhan, 430079, P.R. China
(e-mail: yongjun_zhang@sina.com, {yjzhang, zxzhang, jqzhang}@supresoft.com.cn)

Received: 27 May 2002 / Accepted: 18 September 2003
Published online: 8 June 2004 –

Abstract. A new approach to reconstructing and inspecting the deformation of industrial parts, especially sheetmetal parts based on CAD-designed data and hybrid point-line bundle adjustment with image sequence, is proposed. Nonmetric image sequence and CAD-designed data of parts are used as the source of information. The strategy of our approach is to reconstruct and inspect deformations of parts automatically with image points and line segments extracted from the images. Basic error equation of line photogrammetry and its modified form are addressed in detail. It is shown that when a certain proper weight is selected, adjustment by condition equations and adjustment by observation equations are equivalent for line photogrammetry. A novel hybrid point-line bundle adjustment algorithm is used to reconstruct industrial parts. The proposed hybrid adjustment model can be used in various 3D reconstruction applications of objects mainly composed of points and lines. The developed inspection system is tested with true image data acquired by a CCD camera, and the results are very satisfying.

Key words: Line photogrammetry – Image sequence – 3D reconstruction – Visual inspection – Hybrid point-line bundle adjustment

1 Introduction

Industrial visual inspection is an area that attracts much attention in computer vision as well as close-range photogrammetry communities. Reducing manpower, maintaining high precision and consistency, and time of inspection are the main foci of researchers. Sablatnig [8] proposed a visual inspection approach based on the separation of feature detection and analysis. A stereo vision and specular reflection technique is used by Kosmopoulos and Varvarigou [4] for inspecting gaps on the automobile production line. Two cameras and two infrared LED lamps are used. The precision of inspection is promising.

Along with the development of computer vision, automated visual inspection (AVI) technique has some applications in industry. Two-dimensional AVI has been widely used in printed circuit board (PCB) areas [7]. But most three-dimensional reconstruction and inspection systems are still time-consuming. A CAD-model-based semiautomatic strategy is used by Vosselman [12] in the reconstruction of industrial installations composed mainly of cylinders and T-junctions, but the reconstruction process is extensively interactive and time consuming. For widely used industrial parts mainly composed of line segments such as sheetmetal parts, there is no practical 3D inspection system that can substitute human efforts in deformation inspection and quality control.

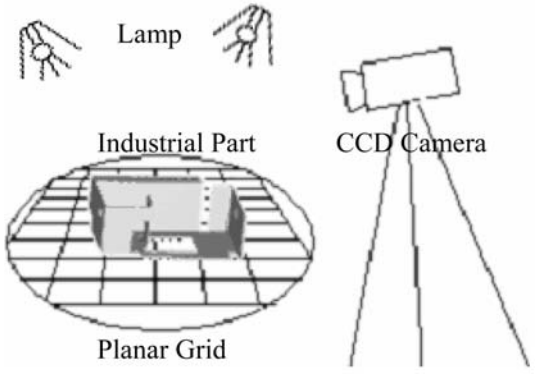

Fig. 1. Overview of inspection system

In this paper, we propose a new approach to reconstructing and inspecting industrial parts based on CAD-designed data and hybrid point-line photogrammetry with image sequence. A sketch of the hardware configuration of our system is shown in Fig. 1. To save on costs, only one CCD camera is used. The light is provided by two house lamps. A planar grid is fixed on a turntable, mainly for camera calibration and offering initial exterior orientation parameters. The sheetmetal part to be inspected is put on the grid.

We start with an overview of the development of line photogrammetry and a general discription of our strategy. In Sect. 3 we discuss the basic mathematical models of both point and line photogrammetry. Proof will be given in Sect. 4 that if a certain weight is selected, adjustment by condition equations can be replaced with adjustment by observation equations for image lines. Then, experiments on the proposed approach are

discussed in detail. Conclusions and the outlook of future developments are given in Sect. 6.

2 Background and general algorithm

2.1 Overview of line photogrammetry

The pine hole camera model is used by traditional point photogrammetry algorithms. Most commercial digital photogrammetry workstations (DPW), which have spurred a large number of successful applications [5,9], are also designed to measure points effectively. But for manmade objects, such as architectures and industrial parts composed mainly of line segments, point photogrammetry is not suitable because few points exist. This leads to the occurrence of line photogrammetry [1,2]. Line photogrammetry focuses on the use of image line observations for accurate object modeling. The most prominent advantage of line photogrammetry is the better automation potential for extraction and measurement of lines in digital imagery. Furthermore, lines have the advantage that they can be only partly visible in an image, and they do not need to be the same part for different images. This means that occluded object points, or object points that are not well defined, can be accurately reconstructed if sufficient lines are available.

In recent years, different line-photogrammetric measurement techniques have been developed. CAD-based line photogrammetry is used by Li and Zhou [6] for measurement of industrial objects. A semiautomatic measurement strategy is used by Streilein and Hirschberg [10] to develop a tool for the generation of 3D CAAD models of architectural objects. An approach to modeling and rendering existing architectural scenes from still photographs is presented by Debevec [2]. Both geometry-based and image-based techniques are adopted in this approach. The reconstruction is an interactive process, and the correspondence between space line and image line is given manually. Another line photogrammetry approach to reconstructing existing architectures represented by polyhedral models has been addressed by van den Heuvel [11]. As in many line-photogrammetric approaches, a parametrization of 3D lines in object space is chosen, and the parameters of the object lines are related to image points on the projection of the lines in the images. This approach uses a polyhedral boundary representation of which point and plane parameters appear in the line-photogrammetric bundle adjustment along with constraints like coplanarity of the points, perpendicularity between faces of the object, and distance constraints between parallel planes.

2.2 General algorithm

Our general strategy is to use a CAD-designed data and hybrid point-line photogrammetry technique to reconstruct and inspect industrial parts quickly and accurately. The CAD data are used as initial values of the final model. The algorithm can be divided into four steps. First, images are acquired by a CCD camera semiautomatically. Then image points and lines are obtained by least-squares template matching. The 3D CAD model of parts is reconstructed accurately with hybrid point-line bundle adjustment in the third step. Unlike existing approaches, the coplanar condition among the projection center, space line, and the corresponding image line is reformed as two equations. Mathematical models of hybrid point-line bundle adjustment are discussed in Sects. 3 and 4. Finally, inspections can be done automatically or interactively. Experimental data and results will be presented in Sect. 5.

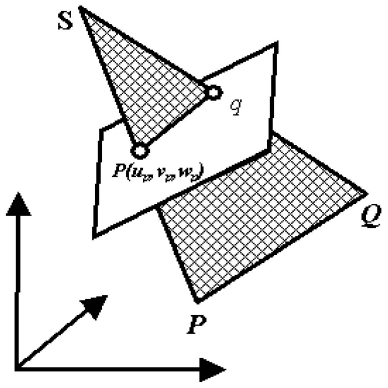

Fig. 2. Coplanarity of image and space lines

3 Basic error equations

3.1 Error equations of line observations

In our approach, the world coordinate system is chosen the same as that of the planar grid. Generally, the CAD-designed coordinate system of the part will not be identical to the world one; there are rotations and translations that must be converted into a unified system. As for the transformation between the part and world, we choose the most widely used form $X' = R \cdot X + T$. R is composed of $(\varphi, \omega, \kappa)$, where Y-axis is taken as the primary axis and T is the translation.

As shown in Fig. 2, the image line *pq*, space line PQ, and projection center S should be coplanar, while p and P, q and Q are not necessarily correspondences, which is the most important advantages of line photogrammetry [2]. A straight line in the image can be parametrized in several ways. Although two parameters suffice for representation of an image line, four image coordinates of two end points are used here because they are singularity free and easy to set up error equations.

In the following line-related equations, (X^0, Y^0, Z^0) represents the coordinate of part point under the part coordinate system, (X, Y, Z) represents its corresponding coordinate under the world system, and $(\Delta X^0, \Delta Y^0, \Delta Z^0)$ is the translation between the part and world system. (X_P, Y_P, Z_P) and (X_Q, Y_Q, Z_Q) are all coordinates of the part points under the world coordinate system. Unlike the existing approaches, the coplanar condition among the projection center, space line, and its corresponding image line is reformed as two equations. The coplanar equation showing the relationship among p, S, P, and Q is

$$\begin{vmatrix} u_p & v_p & w_p \\ X_P - X_S & Y_P - Y_S & Z_P - Z_S \\ X_Q - X_S & Y_Q - Y_S & Z_Q - Z_S \end{vmatrix} = 0\,, \qquad (1)$$

where (u_p, v_p, w_p) is the model coordinate of p and (X_S, Y_S, Z_S) is the coordinate of projection center S. Thus the error equations can be written as follows:

$$\begin{aligned} &A_1 dx_p + A_2 dy_p + A_3 d\varphi + A_4 d\omega + A_5 d\kappa + A_6 dX_S \\ &+A_7 dY_S + A_8 dZ_S + A_9 d\varphi^0 + A_{10} d\omega^0 + A_{11} d\kappa^0 \\ &+A_{12} d\Delta X^0 + A_{13} d\Delta Y^0 + A_{14} d\Delta Z^0 + A_{15} dX_P^0 \\ &+A_{16} dY_P^0 + A_{17} dZ_P^0 + A_{18} dX_Q^0 + A_{19} dY_Q^0 \\ &+A_{20} dZ_Q^0 + F_X = 0\,, \end{aligned} \tag{2}$$

where $A_1 \sim A_{20}$ is the partial derivatives for each unknown term and F_X is the constant item that is the value of determinant of coplanar Eq. 1. In Eq. 1, if $(X'_P, Y'_P, Z'_P) = (X_P - X_S, Y_P - Y_S, Z_P - Z_S)$, $\left(X'_Q, Y'_Q, Z'_Q\right) = (X_Q - X_S, Y_Q - Y_S, Z_Q - Z_S)$, $A = Y'_P \cdot Z'_Q - Y'_Q \cdot Z'_P$, $B = Z'_P \cdot X'_Q - Z'_Q \cdot X'_P$, and $C = X'_P \cdot Y'_Q - X'_Q \cdot Y'_P$ are chosen, we have $F_X = Au_p + Bv_p + Cw_p$.

Besides the coplanar equation showing the relationship among p, S, P, and Q, there is another equation showing the relationship among q, S, P, and Q. The linearized form is similar to Eq. 2.

The unit of constant term $F_X = Au_p + Bv_p + Cw_p$ of the basic error equation for line photogrammetry is not pixel, so it is very difficult to detect gross errors during bundle adjustment. We will deal with this problem in the following discussion.

A space plane can be defined uniquely by three space points, and there exists a constraint condition for the fourth point – the distance from the fourth point to the plane should equal zero. So we may change the constant term of basic error Eq. 2 into the form of the distance between image point (p, q) and the plane defined by the projection center S and space points P, Q.

The plane defined by S, P, and Q can be written in the general form

$$AX + BY + CZ = 0\,, \tag{3}$$

where the definition of A, B, C is the same as that of F_X. If the image point p is coplanar with the plane defined by S, P, Q, the distance $d = 0$, i.e.,

$$d = \frac{A \cdot u_p + B \cdot v_p + C \cdot w_p}{\sqrt{A^2 + B^2 + C^2}} = 0\,. \tag{4}$$

The distance-based error equation can be obtained by taking partial derivatives of Eq. 4. Actually, the numerator of Eq. 4 is identical to the constant term F_X of Eq. 2, so the distance-based error equation can be easily obtained by dividing each term of Eq. 2 with the denominator $\sqrt{A^2 + B^2 + C^2}$.

3.2 Error equations of point observations

For parts that are very simple or there are a few line segments in image, the geometric configuration of image is very poor. In this case, grid points should be combined into the adjusmtent model to ensure the reliability and precision of adjustment. As for grid points, there are no coordinate transformations. Their error equations have the following form [13,5]:

$$\begin{aligned} v_x &= B_1 d\varphi + B_2 d\omega + B_3 d\kappa + B_4 dX_S + B_5 dY_S \\ &\quad +B_6 dZ_S + B_7 dX + B_8 dY + B_9 dZ - l_x \\ v_y &= C_1 d\varphi + C_2 d\omega + C_3 d\kappa + C_4 dX_S + C_5 dY_S \\ &\quad +C_6 dZ_S + C_7 dX + C_8 dY + C_9 dZ - l_y, \end{aligned} \tag{5}$$

where l_x, l_y are the constant items of error equations that can be easily obtained by collinearity equations. The coefficients of error equations $B_1 \sim B_9$ and $C_1 \sim C_9$ are all ommitted in the interest of saving paper; please see [13,5] for more details. If the world coordinates of grid points are treated as known, terms of (dX, dY, dZ) should be removed from the error equations.

4 Model of line photogrammetry

In the previous section, we discussed that if a part is very simple or there are a few line segments in an image, grid points should be combined into an adjusmtent model to ensure the reliability and precision of adjustment. The model of Eq. 2 is adjustment by condition equations with unknowns, while the model of Eq. 5 is adjustment by observation equations. So we should unify them into a single adjustment model to combine the point observations of the grid and line observations of the part together.

The model of adjustment by condition equations for line photogrammetry can be written as the following general form:

$$\begin{cases} A_V V + A_X \delta_X + W = 0 \\ A_X^T K = 0\,, \end{cases} \tag{6}$$

where $V = (dx_p, dy_p, dx_q, dy_q \ldots)$ is the correction vector of the line observations, A_V and A_X the coefficient matrix of vector V and unknowns δ_X such as $A_1 \sim A_{20}$ in Eq. 2, K an intermediate matrix for convenience of adjustment, and W the constant item such as F_X in Eq. 2. The solution vector is

$$\delta_X = -\left(A_X^T N^{-1} A_X\right)^{-1} A_X^T N^{-1} W\,, \tag{7}$$

where $N = A_V P^{-1} A_V^T$ is the normal matrix, with P the corresponding weight matrix.

The error equation and its corresponding normal equation of adjustment by observation equations for point photogrammetry are

$$\begin{aligned} &V = B_X \delta_X + l \\ &B_X^T P' B_X \delta_X + B_X^T P' l = 0\,, \end{aligned} \tag{8}$$

where V is the correction vector, B_X the coefficient matrix of unknowns δ_X such as $B_1 \sim B_9$ and $C_1 \sim C_9$ in Eq. 5, l the constant items such as l_x, l_y in Eq. 5, and P' the corresponding weight matrix. The solution of Eq. 8 is

$$\delta_X = -\left(B_X^T P' B_X\right)^{-1} B_X^T P' l\,. \tag{9}$$

Now, let $B_X = A_X, W = l$; from this it can be seen that the only difference in computing δ_X is the difference between matrix N^{-1} and P' in Eqs. 7 and 9, respectively.

In the previous section, the unit of constant term F_X of line photogrammetry was converted to pixels, which denote the distance between the end point of the image line and the plane defined by the projection center and the space line. If the model of adjustment by condition equations is chosen, two corrections exist for every error equation, and there are no correlations among different equations. The coefficient matrix

A_V can be written as (taking one image line observation as sample):

$$A_V = \begin{pmatrix} \frac{A_{11}}{D} & \frac{A_{12}}{D} & 0 & 0 & \dots \\ 0 & 0 & \frac{A_{21}}{D} & \frac{A_{22}}{D} & \dots \\ \dots & & \dots & & \dots, \end{pmatrix} \quad (10)$$

where (A_{11}, A_{12}) and (A_{21}, A_{22}) are the coefficients of the corrections (dx_p, dy_p) and (dx_q, dy_q) of the two end points of an image line, respectively. $D = \sqrt{A^2 + B^2 + C^2}$, and the definition of (A, B, C) is the same as Eq. 4. The normal matrix is $N = A_V P^{-1} A_V^T$, and its inverse is $N^{-1} = \left(A_V P^{-1} A_V^T\right)^{-1}$.

It can be seen that only diagonal terms are not equal to zero in matrix N^{-1}. So if $P' = N^{-1}$ is selected as the weight matrix for Eq. 9, the line bundle adjustment model (Eqs. 6 and 7) can be replaced with adjustment by observation equations (Eqs. 8 and 9). Thus we can take hybrid point-line bundle adjustment under a single model of adjustment by observation equations.

5 Experiments

A software program called VisualInspector, which runs quickly and automatically, has been developed according to the above algorithms to reconstruct and inspect the deformation of industrial parts composed mainly of points and lines. The proposed approach has been tested with real image data of many sheetmetal parts taken by a precalibrated CCD camera with a resolution of 1300×1030 pixels. All inspection results are very promising, and one of the typical results will be discussed in the following discussion.

As described in Sect. 2, our whole inspection procedure at present includes four steps. First, the image sequence is acquired by CCD digital camera semiautomatically because the rotation table cannot be controlled by computer. Our inspection software can do the next three steps fully automatically. Image points of the grid and lines of the part are obtained in the second step by least-squares template matching. Then a 3D CAD model of parts is reconstructed accurately with hybrid point-line bundle adjustment. And finally, inspections can be done automatically or interactively. Each step will be explained in the following discussion.

In the first step, a sequence of 25 images is taken. The CCD camera with a 25-mm lens used here has been calibrated with the planar grid in advance [14]. The camera is fixed on a tripod at a distance of about 600 mm to the part. The industrial sheetmetal part with a dimension of about 150 mm to be inspected is put on the planar grid, which is fixed on the turntable, as shown in Fig. 1. Images are obtained by the CCD camera with equal angle intervals while the human-controlled table turns around its rotating center.

Image points and lines are extracted automatically in the second step. Image points of the grid are detected as the intersection of straight lines fitted to each cross with a precision of more than 0.05 pixels. As shown in Fig. 3, the black crosses are the predicted image corners, and the white ones are the matched corners with a least-squares template matching technique [3].

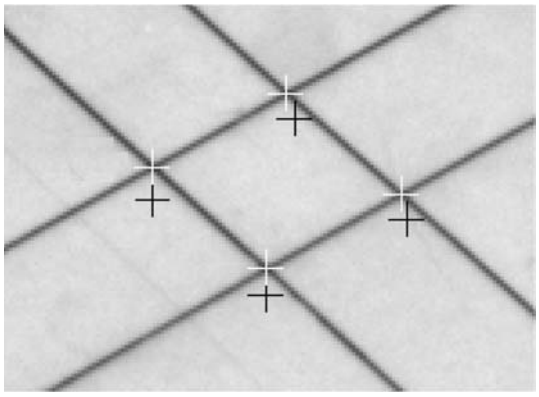

Fig. 3. Predicted and matched image points of the grid

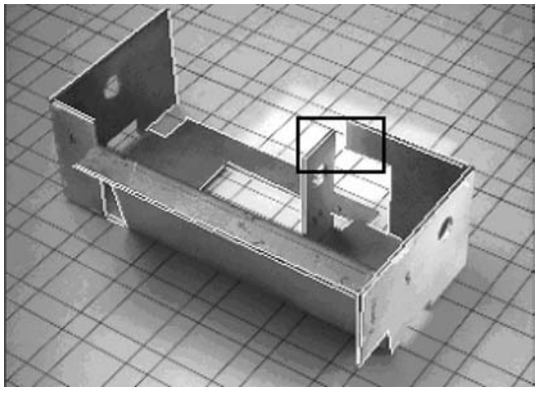

Fig. 4. The first image used for inspection

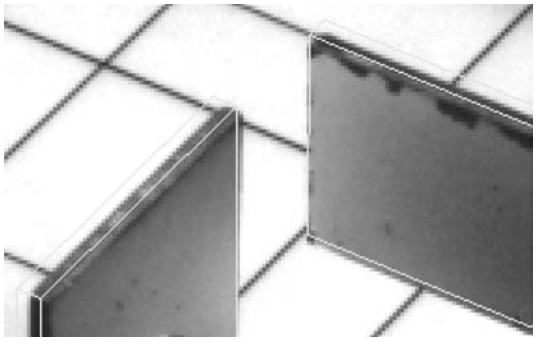

Fig. 5. Predicted image lines of part

Image lines corresponding to each space line of the part are also obtained fully automatically with least-squares template matching in a local search window. Initial values of end points of image line segments are projected by the CAD-designed data and the camera parameters offered by the grid. A small image block containing the part in the first image is shown in Fig. 4. White lines in Fig. 4 are the matched line segments. The predicted and matched grid points are similar to Fig. 3 and therefore not shown in Fig. 4.

The small window in the rectangle of Fig. 4 is enlarged in Figs. 5 and 6 for more detail. Figure 5 shows the initial projection of line segments of the part. As can be seen, the projected initial image lines are usually several pixels away from the real image edges of the part. Although there are many rust spots on the part that can be seen clearly in Fig. 5, the matched image lines are well fitted to the real image edges, as

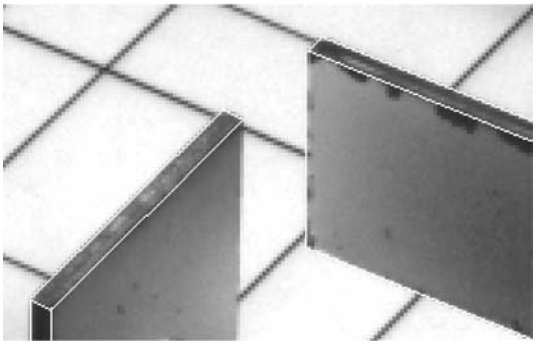

Fig. 6. Matched image lines of part

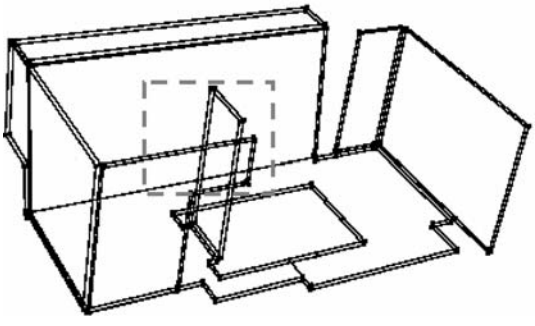

Fig. 7. 3D view of reconstructed model

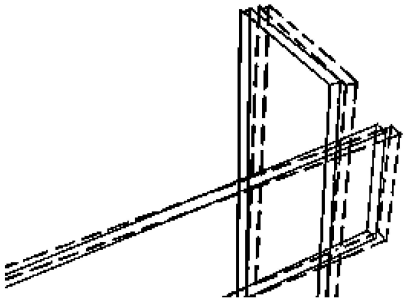

Fig. 8. Comparison of reconstructed and raw CAD model

shown in Fig. 6. Thus the problem of correspondence between space edges and image line segments is resolved successfully.

In the third step, a hybrid point-line bundle adjustment model is used to reconstruct the industrial parts. The CAD-designed data offer not only initial values of line segments of the part but also the topological geometry. During the hybrid bundle adjustment, the CAD-designed coordinates of space points are used as initial values. The designed corners of the planar grid are measured with a coordinate measuring equipment with a precision of about 0.1 mm. Thus the measured coordinates of the grid are treated as weighted unknowns.

It takes about 30 s to get the 3D CAD model of the part in a PIV personal computer. The output of our inspection system is the accurately reconstructed 3D CAD model of the part that can be used for deformation inspection automatically or interactively. A 3D view of the reconstructed wire-frame model visualized with OpenGL is shown in Fig. 7. As for the small section shown as a dashed rectangle in Fig. 7, a comparison of the reconstructed and raw CAD models of the part is shown in Fig. 8. The real line segments are the reconstructed model, and

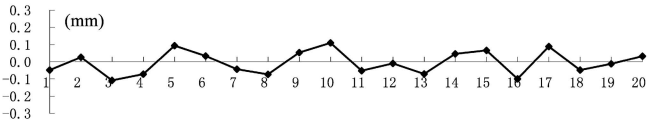

Fig. 9. Deviations between reconstructed and measured distances

the dashed line segments are the raw CAD model. As can be seen, there are significant differences between the two models.

To check the precision of the proposed reconstruction and inspection system, 20 distances between lines and planes on the sheetmetal part are measured manually and compared with measurements computed by the reconstructed model. The results are shown in Table 1. Here "Designed" means CAD-designed distances between lines, planes, or lines to planes. "Measured" means corresponding distances measured manually by calipers. "Computed" means distances computed with the reconstructed model. "MD" and "CD" represent measured and computed deformations, respectively. "Deviation" indicates the differences between computed and measured deformations.

Table 1 shows that the largest deformation of the part is about 0.5 mm, and all deformations larger than 0.1 mm can be detected accurately by our system. When the computed deformations subtract the corresponding measured deformations, i.e., the measured deformations are treated as zero, the deviations show a well normal distribution, as shown in Fig. 9.

The RMS error of deviations is 0.07 mm. The relative precision, which can be calculated as the ratio of RMS against the distance between camera and the part, is about 1/8500 (0.07 mm/600 mm = 1/8500). This shows the precision of our inspection system when measured distances are treated as errorless. Furthermore, distances measured manually by calipers cannot be errorless, so the actual precision of the proposed reconstruction and inspection system should be even higher. As can be seen, the precision of our system is higher than

Table 1. Distances measured and computed (mm)

No.	Designed	Measured	Computed	MD	CD	Deviation
1	50.200	49.700	49.652	−0.500	−0.548	−0.048
2	50.200	49.700	49.726	−0.500	−0.474	0.026
3	20.000	19.960	19.852	−0.040	−0.148	−0.108
4	36.000	36.000	35.928	0.000	−0.072	−0.072
5	60.000	60.000	60.093	0.000	0.093	0.093
6	60.000	60.000	60.034	0.000	0.034	0.034
7	51.600	51.400	51.357	−0.200	−0.243	−0.043
8	53.200	53.020	52.947	−0.180	−0.253	−0.073
9	54.800	54.500	54.554	−0.300	−0.246	0.054
10	99.800	100.100	100.210	0.300	0.410	0.110
11	49.400	49.200	49.148	−0.200	−0.252	−0.052
12	153.000	153.200	153.190	0.200	0.190	−0.010
13	149.800	150.000	149.926	0.200	0.126	−0.074
14	14.500	14.500	14.546	0.000	0.046	0.046
15	9.600	9.600	9.666	0.000	0.066	0.066
16	15.000	15.000	14.902	0.000	−0.098	−0.098
17	34.400	34.000	34.089	−0.400	−0.311	0.089
18	33.200	33.400	33.352	0.200	0.152	−0.048
19	22.000	22.360	22.348	0.360	0.348	−0.012
20	76.400	76.100	76.132	−0.300	−0.268	0.032

that of Kosmopoulos and Varvarigou [4], which can achieve a precision of 0.1 mm within an area of 80 mm × 80 mm. Furthermore, the cost of hardware configuration of our system is cheaper than that of Kosmopoulos and Varvarigou [4].

The hybrid point-line adjustment model proposed in this paper has also been used as a basic algorithm in 3D city model generation. Buildings composed mainly of points and lines can be easily reconstructed with this technique. Intermediate results, which are very promising, are presented by Zhang et al. [15].

6 Summary and outlook

A novel approach to reconstructing and inspecting the deformation of industrial parts, especially sheetmetal parts based on hybrid point-line bundle adjustment with image sequence, is presented. Unlike the existing approaches, the coplanar condition among the projection center, space line, and its corresponding image line is reformed as two equations. It is shown that when a certain proper weight matrix is selected, adjustment by condition equations and adjustment by observation equations are equivalent for line photogrammetry. The hybrid point-line bundle adjustment model is adopted to reconstruct the industrial parts. The proposed approach is tested with true image data taken with a precalibrated CCD camera, and the results are very satisfying. The developed inspection system runs automatically and quickly, which shows it to be a promising approach to replacing human beings in deformation inspection or quality control of assembly lines.

Full automation of inspection will be the main focus of our work in the near future. The rotation table used at present will be replaced by a new computer-controllable one, and image matching will be done simultaneously with automatic image acquiring. A matching process will be activated once a new image comes. This improvement will realize full automation and reduce the total time of inspection significantly.

Acknowledgement. This work is supported by National Natural Science Foundation of China under contract number 40301041.

References

1. Baillard C, Schmid C, Zisserman A et al (1999) Automatic line matching and 3D reconstruction of buildings from multiple views. Int Arch Photogramm Remote Sens 32:69–80, Part 3-2W5
2. Debevec PE (1996) Modelling and rendering architecture from photographs: a hybrid geometry- and image-based approach. In: Proceedings of SIGGRAPH
3. Gruen A (1985) Adaptive least square correlation: a powerful image matching technique. South Afr J Photogramm Remote Sens 14(3):175–187
4. Kosmopoulos D, Varvarigou T (2001) Automated Inspection of gaps on the automobile production line through stereo vision and specular reflection. Comput Ind 46(1):49–63
5. Kraus K (1993) Photogrammetry, vol 1: Fundamentals and standard processes. Dümmlers, Bonn
6. Li D, Zhou G (1994) CAD-based line photogrammetry for automatic measurement and reconstruction of industrial objects. Int Arch Photogramm Remote Sens 30(5):231–240
7. Moganti M, Ercal F, Dagli Ch et al (1996) Automatic PCB inspection algorithms: a survey. Comput Vision Image Understand 63(2):287–313
8. Sablatnig R (1996) Flexible automatic visual inspection based on the separation of detection and analysis. In: Proceedings of ICPR
9. Schenk T (1999) Digital photogrammetry. TerraScience, Laurelville, OH
10. Streilein A, Hirschberg U (1995) Integration of digital photogrammetry and CAAD: constraint-based modelling and semi-automatic measurement. In: Proceedings of the CAAD Futures '95 international conference, Singapore
11. van den Heuvel FA (1999) A line-photogrammetry mathematical model for the reconstruction of polyhedral objects. Proc SPIE 3641:60–71
12. Vosselman G (2001) Semi-automatic CAD based reconstruction of industrial installations. Künstliche Intelligenz 4:23–27
13. Wang Z (1990) Principles of photogrammetry. Publishing House of Surveying and Mapping, Beijing, PR China
14. Zhang Y, Zhang Z (2003) Camera calibration technique with planar scenes. In: Proceedings of the 11th conference on machine vision applications in industrial inspection at IS&T/SPIE Electronic Imaging, Santa Clara, CA, 20–24 January 2003, 5011:291–296
15. Zhang Y, Zhang Z, Zhang J (2003) Multi-view 3D city model generation with image sequences. In: Proceedings of the 6th AGILE conference on geographic information science, Lyon, France, pp 697–701

Yongjun Zhang received his ME degree in Geodesy from Wuhan Technical University of Surveying and Mapping in 2000 and his PhD in Photogrammetry and Geomatics from Wuhan University in 2002, P.R. China. He was a guest researcher of Institute for Photogrammetry and GeoInformation, University of Hannover during 2003. Now he is an associate professor in Wuhan University, P.R. China. His research interests include Digital Photogrammetry and Computer Vision.